Magnetic and metal-insulator transitions in coupled spin-fermion systems

R. Mondaini, T. Paiva, and R. T. Scalettar

Phys. Rev. B **90**, 144418 — Published 14 October 2014

DOI: 10.1103/PhysRevB.90.144418

Magnetic and metal-insulator transitions in coupled spin-fermion systems

R. Mondaini[1,2], T. Paiva[3], and R.T. Scalettar[2]
[1] *Physics Department, The Pennsylvania State University, 104 Davey Laboratory, University Park, Pennsylvania 16802, USA*
[2] *Physics Department, University of California, Davis, California 95616, USA and*
[3] *Instituto de Física, Universidade Federal do Rio de Janeiro Cx.P. 68.528, 21941-972 Rio de Janeiro RJ, Brazil*

We use quantum Monte Carlo to determine the magnetic and transport properties of coupled square lattice spin and fermionic planes as a model for a metal-insulator interface. Specifically, layers of Ising spins with an intra-layer exchange constant J interact with the electronic spins of several adjoining metallic sheets via a coupling J_H. When the chemical potential cuts across the band center, that is, at half-filling, the Néel temperature of antiferromagnetic ($J > 0$) Ising spins is enhanced by the coupling to the metal, while in the ferromagnetic case ($J < 0$) the metallic degrees of freedom reduce the ordering temperature. In the former case, a gap opens in the fermionic spectrum, driving insulating behavior, and the electron spins also order. This induced antiferromagnetism penetrates more weakly as the distance from the interface increases, and also exhibits a non-monotonic dependence on J_H. For doped lattices an interesting charge disproportionation occurs where electrons move to the interface layer to maintain half-filling there.

PACS numbers: 71.10.Fd, 71.30.+h, 02.70.Uu

I. INTRODUCTION

Over the last several decades an extensive literature has developed describing Monte Carlo simulations of both localized (e.g. Heisenberg) and itinerant (e.g. Hubbard) models of quantum magnetism. An important subset of these studies has considered situations where the exchange constants J_α or electron repulsion U_α can take on multiple values, with the attendant possibility of quantum phase transitions as the ratio of these energy scales is altered. For example, in the case of the one-fifth depleted square lattice model of CaV_4O_9, the quotient J/J' of the exchange constants on the two different vanadium bonds tunes the associated Heisenberg hamiltonian from a disordered dimer phase, to Néel order, and then back to a disordered plaquette phase[1], lending an understanding of spin gapped behavior in this material. Likewise, bilayer Heisenberg[2] and Hubbard[3] models have a singlet to Néel transition depending on the ratio of values of the inter- and intra-plane energies.

In addition to describing systems in which long range order can be destroyed, multiple J_α and U_α can also give rise to transitions between different ordered states, such as charge density versus spin density wave patterns. Simulations of models with several interaction energy scales are especially relevant to heterostructures, where the growth of distinct sheets of the same, or different materials, offers the possibility of tuned magnetic properties.

In this paper we present a quantum Monte Carlo investigation of a mixed localized-itinerant magnetic model in which we couple a 2D square layer of Ising spins to several metallic planes. Our interest is both in how, potentially, the additional fluctuations of the free electrons suppress the Ising transition temperature and on how the magnetic layer initiates order amongst the free fermions. We also explore whether the coupling of the metal to the localized spins can open a gap in the electronic spectrum, driving a metal to insulator transition, and the penetration depth of the magnetic order into the metal. Our work is related to simulations of multilayer Hubbard models in which the on-site interaction U can distinguish metallic from magnetic layers[4]. However, by treating the correlated layers as classical, localized spins we are able to explore a greater range of parameter space, and, in particular, to go to lower temperatures away from half-filling of the metallic band where a sign problem would otherwise prevent simulations.

This idea of coupling classical spins to itinerant electrons has been extensively used, e.g. in multiband models of the manganites and iron pnictides where the sign problem similarly precludes treating fully quantum mechanical models[5–7]. Numerical approaches to these models allow easier access to dynamical behavior and hence greater possibility of contact with spectroscopy and neutron scattering experiments[8] than do direct path integral treatments of many-electron systems which require a difficult analytic continuation to get real time information.

A number of recent experiments have examined electronic reconstruction at the interface of different transition metal oxides using scanning tunneling microscopy with high spatial and energy resolution. Some of these experiments focus on interfaces of paramagnetic metals and antiferromagnetic insulators[9–11]. The Hamiltonian we consider here, in which tight binding layers couple to classical, localized spins, is the most simple model of such a situation, and will clearly require considerable refinement before being able to make any sort of quantitative contact. Nevertheless, it can lend a first qualitative insight into the sort of trends one might expect, e.g. for magnetic

order. Moreover, the study of fluctuating classical spins coupled to fermionic degrees of freedom has recently been suggested as a generally promising approach to move beyond mean-field treatments of interacting electron systems[12], providing further motivation for this work.

The remainder of this paper is organized as follows: In Sec. II we write down the fermion-Ising hamiltonian along with a brief summary of the numerical methods employed, and definitions of the observables which characterize the phases. Section III describes the results when the Fermi level is at the band center, first for the case of antiferromagnetic (AF) Ising spins and then for ferromagnetic coupling, followed by a discussion (Sec. IV) of the effect of doping away from half-filling. A particular interesting charge disproportionation is shown to occur where metallic layers become unequally populated to allow for an optimal magnetic response. Section V presents a conclusion and some future directions of research.

II. MODEL

We consider the hamiltonian

$$\begin{aligned}\hat{H} = &-t \sum_{\langle ij\rangle \ell,\sigma} \left(c^\dagger_{i\ell\sigma} c_{j\ell\sigma} + c^\dagger_{j\ell\sigma} c_{i\ell\sigma} \right) - \mu \sum_{i\ell,\sigma} n_{i\ell\sigma} \\ &-t_\perp \sum_{i\langle \ell\ell'\rangle,\sigma} \left(c^\dagger_{i\ell\sigma} c_{i\ell'\sigma} + c^\dagger_{i\ell'\sigma} c_{i\ell\sigma} \right) \\ &-J_H \sum_i s^z_{i,\ell=0}\, S_i + J \sum_{\langle ij\rangle} S_i\, S_j, \end{aligned} \tag{1}$$

where $c^\dagger_{i\ell\sigma}\,(c_{i\ell\sigma})$ are creation(destruction) operators for fermions of spin σ on lattice site i of layer $\ell = 0, 1, \cdots, N_{\rm layer}-1$. Our convention is that layer $\ell = 0$ is adjacent to the classical spins. The intra-layer hopping t is on nearest-neighbor sites (denoted by $\langle ij\rangle$) of each layer ℓ; the inter-layer hopping between neighboring fermionic layers $\langle \ell\ell'\rangle$ is $t_\perp$, and the density of fermions is tuned by the chemical potential μ. The geometry of each layer is that of a 2D square lattice of linear length L. The remaining degrees of freedom are Ising spins which populate a single layer[13] and are coupled by exchange constant J. The Ising spins interact with the z component of the fermion spin $s^z_{i,0} = n_{i,0,\uparrow} - n_{i,0,\downarrow}$ in the interface layer $\ell = 0$, via a second exchange constant, J_H. The lattice geometry is sketched in Fig. 1. We choose periodic boundary conditions in the planes, and open boundary conditions in the direction perpendicular to the planes. Our results will be for two metallic layers (i.e. $N_{\rm layer} = 2$), since, as we shall show, such a situation already allows us to address many of the key questions concerning the interface between a magnetic and a metallic layer.

We have chosen $|J|/t = 0.2$ (both signs of J will be studied) so that the temperature scale for the development of correlations in the classical spins is comparable to that in the metallic layer and, consequently, possible competing phases are most readily discerned. There are different ways to understand this. The most simple is to note that, if $J = t$, the 2D square lattice Ising $T_c \sim 2.27J$ is much higher than typical temperature scales at which short range correlations get more robust for noninteracting fermions in a square lattice. This is because for the half-filled $U = 0$ Hubbard Hamiltonian, short range antiferromagnetic correlations corresponding to the Fermi wavevector is $\mathbf{k}_F = (\pi, \pi)$, do not onset until the temperature gets below $T \sim 0.25t$. Even when electron-electron interactions, which are not considered here, are turned on, nearest neighbor spin correlations do not begin to grow substantially until $T \sim 0.5t$ (for the $U/t = 4$ Hubbard model). Thus in either case, a choice $|J|/t \sim 0.2$ (Ising $T_c \sim 0.45t$) is required to select classical spin and fermionic spin ordering scales to be roughly equal.

An alternate to Eq. 1 would be to consider continuous planar $\vec{\mathbf{S}} = (S^x_i, S^y_i)$ or Heisenberg $\vec{\mathbf{S}} = (S^x_i, S^y_i, S^z_i)$ spins, with an $\vec{\mathbf{S}}_i \cdot \vec{\mathbf{S}}_j$ spin-spin coupling between pairs of local spins, and $\vec{\mathbf{S}}_i \cdot \vec{\mathbf{s}}_j$ spin-spin of local spin to fermion spin.[5] The restriction used here, to a single (z) component, has been considered in other problems involving treating electronic correlation, from mean field approaches[14] to the study of the t-J_z model.[15] The choice of Ising spins also ensures a robust magnetic phase transition in which true long range order occurs at finite T_c in the spin plane. This will be discussed further in the conclusions.

It is worth noting several symmetries of the hamiltonian Eq. 1. Consider first a combined particle-hole transformation $c_{i\sigma} \rightarrow (-1)^i c^\dagger_{i\sigma}$ and inversion of the localized spins $\left(S_i \rightarrow -S_i \right)$. Here $(-1)^i$ denotes a staggered ± 1 phase taking opposite values on the two sublattices of the bipartite square lattice. This transformation leaves each of the terms in the hamiltonian- the fermion kinetic energy, the Ising interaction, and the local spin-fermion coupling invariant. Thus, if $\mu = 0$, the whole hamiltonian is unchanged, and the lattice is half-filled ($\rho = 1.0$).

The finite temperature properties of the system can be obtained from its partition function and associated expectation values. The partition function is,

$$Z = \sum_{S_i = \pm 1} e^{\beta J \sum_{\langle ij\rangle} S_i S_j} \cdot Z_{\rm f}(\{S\}), \tag{2}$$

where $Z_{\rm f}(\{S\}) = {\rm Tr}\, e^{-\beta(\hat{H}_{\rm f\uparrow} + \hat{H}_{\rm f\downarrow})}$ represents the grand-canonical partition function of the fermionic part of the hamiltonian for a particular Ising field configuration $\{S\}$. Since the hamiltonian Eq. 1 is bilinear in the fermionic operators, each $\hat{H}_{{\rm f}\sigma}$ can be written as the product of a vector of creation operators, a real-valued matrix $\mathcal{M}^\sigma$,[16] and a vector of destruction operators. The fermion contributions to Z can then be expressed in terms of the

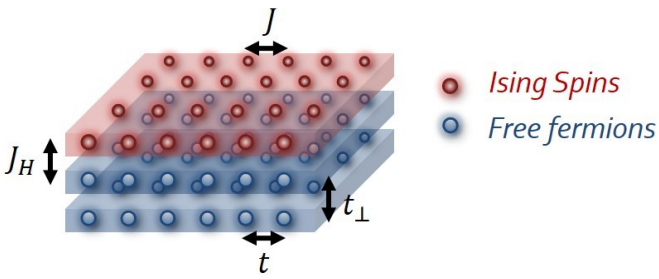

FIG. 1. (Color online) Lattice geometry for the fermion-Ising model. A single layer of Ising spins residing on a 2D square lattice is superposed on several layers of noninteracting fermions. The nearest-neighbor spin-spin interaction between the free fermions of layer $\ell = 0$ and the Ising spins is proportional to the parameter J_H.

eigenvalues λ_j^σ of $\mathcal{M}^\sigma$,

$$Z_{\rm f} = \prod_{\sigma=\uparrow,\downarrow} \prod_j \left(1 + e^{\beta\lambda_j^\sigma}\right). \tag{3}$$

From this expression, it is clear that the summand in Eq. 2 is positive definite and there is no "sign problem" (for any μ). Of course, this is simply a consequence of the fact that the spin field to which the fermions are coupled does not vary in imaginary time, as it would, for example, if $\{S\} = S_{i\tau}$ were a Hubbard-Stratonovich field used to decouple a fermion-fermion interaction. The largest computational effort arises from diagonalizing the two NxN matrices $\mathcal{M}^\sigma$ for each update to the configuration of the Ising spins S_i.

An alternate method to the direct matrix diagonalization used in the literature employs a representation of the density of states $\rho(\lambda)$ in terms of Chebyshev polynomials[17–19]. The moments of $\rho(\lambda)$ are computed recursively in a way that involves only sparse matrix-vector multiplications. This approach improves the scaling with system size to linear in N, at the cost of a significant prefactor. It also involves a (well-controlled) approximation which is the truncation of the expansion at some maximum order. Here we use exact diagonalization, as opposed to the Chebyshev method.

The results of the simulations presented below were obtained by averaging over 5-10 independent simulations, each of which was composed of 35,000 Monte Carlo sweeps of the Ising variables. Typically, the linear lattice size L was varied between $4 \le L \le 12$, selecting a geometry with one Ising plane and stacked on top of two fermionic ones, so that $N = 2\,L^2$.

Expectation values of the Ising variables are averaged in the usual way over the configurations generated in the course of the simulation. For example, to address directly if there is long range ferromagnetic order in the Ising plane in the case $J < 0$, we calculate the fourth order Binder cumulant[20], $B_4(T) = \left(1 - \langle M^4\rangle/3\langle M^2\rangle^2\right)$. Here $M = 1/N\sum_i S_i$ is the magnetization per site. When $J > 0$ (the antiferromagnetic case) we replace M by the staggered magnetization, $1/N\sum_i (-1)^i S_i$. Crossings of $B_4(T)$ obtained for different lattice sizes determine the critical temperature for magnetic ordering of the classical spins. When the interaction J_H between the Ising and fermionic spins is nonzero, we expect a shift away from the 2D square lattice Ising $T_c = 2.269\,|J|$.

Fermionic measurements like the kinetic energy, double occupancy, and spin-spin correlations can be written in terms of combinations of the single particle Green's functions, $G_{ij}^\sigma = \langle\, c_{i\sigma} c_{j\sigma}^\dagger \,\rangle = (\mathcal{M}_{ij}^\sigma)^{-1}$, for every configuration of the classical spins. The elements of G^σ are easily obtained from the diagonalization of $\mathcal{M}^\sigma$ which is already in hand from the update of the spin variables. Further details of the numerical algorithm for coupled classical spin-fermion systems are contained in Refs. [5, 17, and 19].

It is known from related simulations of Hubbard hamiltonians that fermions with no direct interaction U have large finite size effects: the discrete (and often highly degenerate) $U = 0$ energy levels $E(k_x, k_y)$ are readily visible in measurements, especially dynamic quantities like the density of states. Although the $U = 0$ metal considered here is coupled to classical spins, and hence does have interactions, we still observe significant finite size effects, especially in the metallic portions of the phase diagram. We overcome this difficulty through the introduction of a small magnetic field $B = \Phi_0/L^2$ along the direction perpendicular to the planes. Here Φ_0 is the magnetic flux quanta. With this choice, the intralayer hopping terms are changed by a Peierls-like phase factor $\left(t_{\mathbf{ij}} \to t\exp\left(\frac{2\pi i}{\Phi_0}\int_{\mathbf{i}}^{\mathbf{j}} \mathbf{A}\cdot d\mathbf{l}\right)\right)$. We use the Landau gauge in order to set the values of the vector potential $\mathbf{A}$. This procedure can be considered as an improvement/generalization of "boundary condition averaging"[21–23]. For a more complete description, see Ref. [24]. Nevertheless, it is important to emphasize the distinction of this field, which couples to the 'orbital' motion of the electrons (i.e. their hopping) from a Zeeman field coupling to spin which affects magnetic order. The orbital field introduced here reduces finite size effects by introducing an additional averaging over discrete allowed momenta on a finite lattice. The coupling to the classical spins, on the other hand, produces a Zeeman field for the electrons, whose role in ordering we will determine.

This reduction in the finite size effects is especially evident in the single particle density of states,

$$N(\omega) = \frac{1}{N}\,{\rm Im}\sum_r \sum_j \frac{|U_{j,r}|^2}{\lambda_j - \omega - i\delta}. \tag{4}$$

Here $U_{j,r}$ are the components of the eigenvectors corresponding to the eigenvalue λ_j of the matrices $\mathcal{M}^\sigma$ defining the (quadratic) hamiltonian, and which now contain the phase factors described above. The outer

sum averages all the equivalent sites in order to recover translationally invariance. Instead of displaying well-separated discrete delta-function peaks, even for free fermions $N(\omega)$ becomes nearly continuous on relatively small lattices, and has a form much closer to that of the thermodynamic limit.[24] In our hamiltonian, turning on J_H further reduces residual finite size effects.

III. RESULTS- HALF-FILLING

Because of Fermi surface nesting with vector $\mathbf{k} = (\pi, \pi)$, the dominant magnetic instability of the half-filled square lattice Hubbard hamiltonian is antiferromagnetic. Indeed, the noninteracting susceptibility $\chi_0(\pi, \pi)$ diverges as temperature $T \to 0$ so that, within the Random Phase Approximation (RPA), the ground state exhibits AF order for any finite U. Similarly, in the strong coupling (Heisenberg) limit, the exchange interaction J favors near neighbor spins which are anti-aligned. Since the $U = 0$ fermion sheets exhibit this strong AF preference, we expect a rather different response to the coupling of an AF versus a F Ising plane to the metal. We begin with the AF case.

A. The antiferromagnetic case

Figure 2 shows the Binder ratio $B_4(T)$ for two metallic planes of linear size L=4, 6, 8, 10 and 12 coupled in each case to a single Ising plane of the same dimensions. The interlayer hopping between the fermionic layers is set to $t_\perp = t$ and the coupling J_H between the local spins and the fermions is $J_H = 3t$. The Binder ratios for the three lattice sizes cross at a common point, $T_c \sim 0.62$, representing a 36% enhancement over the free spin plane result $T_c \sim 2.27J = 0.454$ for $J = 0.2$.

Similar Binder crossing plots for other choices of J_H and interlayer hopping yield analogous transition temperatures, which are shown in Fig. 3. The enhancement in T_c over that of an independent spin plane is nontrivial, because there is a competition between the additional entropy which results from fluctuations of fermionic variables in the metallic plane and the tendency, noted above, towards antiferromagnetism of the $U = 0$ Hubbard model, due to Fermi surface nesting. Evidently, the latter tendency wins: $T_{\text{Néel}}$ is enhanced. The universality class of the transition to an ordered phase as the temperature is lowered remains an open question. Our results are consistent with an Ising transition, and we believe that is the most likely scenario, but the available system sizes do not allow us to draw any final conclusion.

There are several additional interesting features in the data. First, the enhancement in T_c is non-monotonic in J_H. The transition temperature reaches a maximum at $J_H/t \sim 3$ for both $t_\perp = 0$ and $t_\perp = t$. Although data are not shown, even for $t_\perp = 5t$ the enhancement of T_c

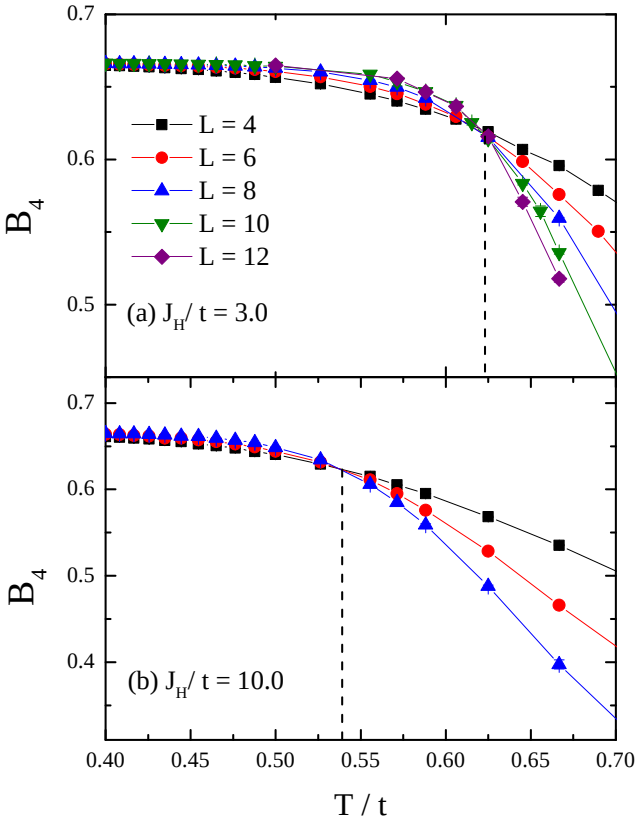

FIG. 2. (Color online) Crossing plot of the Binder ratio of an AF Ising sheet coupled with $J_H = 3t$ (top) and $J_H = 10t$ (bottom) to two metallic layers. The interlayer hopping between the fermion layers was set to $t_\perp = t$. For $J_H = 3t$, the crossing occurs at $T/t \sim 0.62$, which is well above the critical temperature of a free Ising sheet ($J_H = 0$). $T/t = (J/t) \cdot (T_c/J) = 0.2 \cdot 2.269 = 0.454$. The behavior of T_c with J_H is nonmonotonic as the critical temperature for $J_H = 10t$ drops to $T/t \sim 0.54$ (see Fig. 3).

comes back down at large J_H. We note that the band structure of the two sheet Hubbard model is $\epsilon(k_x, k_y) = -2t\big(\cos k_x + \cos k_y\big) \pm t_\perp$. The two bands overlap for $t_\perp < 4t$ and have a band gap $t_\perp - 4\,t$ otherwise. Thus the choice $t_\perp = 5\,t$ represents the coupling of an Ising spin layer to a band insulator rather than a metal. Figure 3 indicates that the magnetic response of the Ising layer is qualitatively the same in the two situations (metal with $t_\perp < 4t$ or band insulator with $t_\perp > 4t$), although the response of a coupling to a band insulator produces less of an effect, as might be expected. This is likely due to the fact that the bilayer Fermi surface is still nested with $\mathbf{k} = (\pi, \pi)$ for $t_\perp > 4\,t$, even though the density of states at E_F vanishes.

The non-monotonic behavior of T_c with J_H is reflected also in the evolution of the farthest-neighbor intraplane

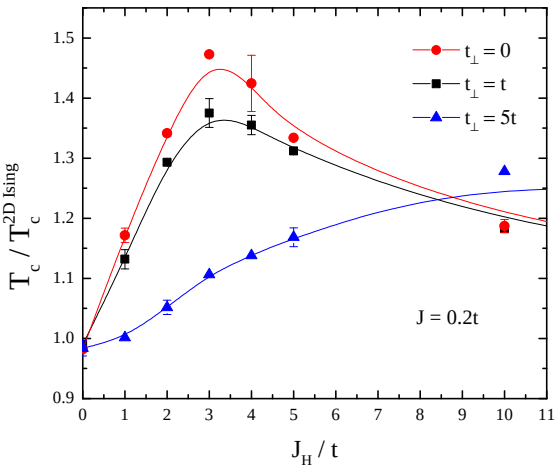

FIG. 3. (Color online) Critical temperature T_c (normalized to the 2D Ising value) for the magnetic transition in the Ising spin plane as a function of the interaction J_H with the metal. Several different choices of the hopping parameter $t_\perp$ connecting the two metallic planes are shown. T_c is obtained by the crossing of the Binder ratio $B_4(T)$ for different lattice sizes. (See Fig. 2.) Coupling of the spin layer to the metal enhances T_c. The degree of enhancement is strongest when the fermionic layers are most weakly coupled to each other (small $t_\perp$). Lines are guides only.

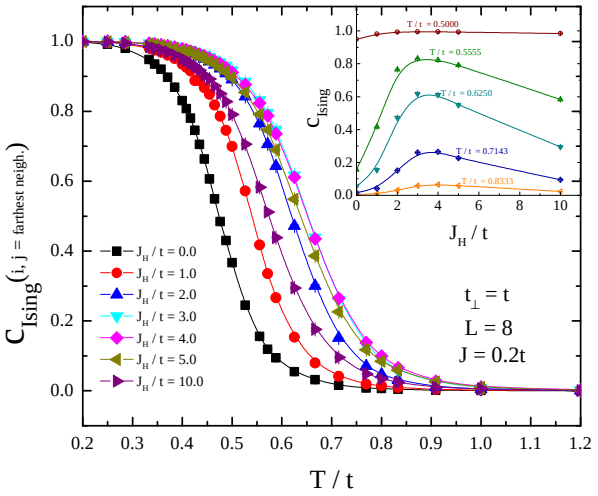

FIG. 4. (Color online) Temperature dependence of the Ising spin-spin correlation between most distant neighbors in the lattice and several values of the interaction J_H for $L = 8$ with one Ising layer stacked over two fermion ones. These correlations display a similar trend to the critical temperature: they initially become more robust with the coupling between the different planes; for large J_H, they return to values similar to the decoupled Ising model ($J_H = 0$). The inset shows the same but now as a function of J_H where the non-monotonic effects on the Ising spins correlations are unequivocal.

spin correlation function. $c(i,j) = \langle S_i S_j \rangle$. Fig. 4 shows $c(i,j)$ vs. T/t for several values of J_H at $t_\perp = t$ on a 8x8 lattice. This quantity, which in the thermodynamic limit would equal the square of the order parameter, evolves rather sharply from zero to one as T/t is lowered. The position where the switch in values occurs moves to larger T/t as J_H changes from $J_H = 0$ to $J_H/t \sim 3-4$, but then comes back down, in agreement with the maximal T_c in Fig. 3. The inset of Fig. 4 displays the same quantity as a function of temperature and shows, unequivocally, this non-monotonic effect.

Having described the effect of the interaction J_H between the Ising spin plane and the metal on the ordering transition of the classical spins, we turn now to the issue of the effect of J_H on the metal. We calculate several quantities that characterize both the magnetism and the transport in the fermionic planes. We begin by showing, in Fig. 5, the intra-plane kinetic energy[25] as a function of temperature for the different values of J_H. In (a), which gives the kinetic energy of electrons in the fermionic plane right at the interface, the increase of the interaction with the Ising spins localizes the electrons, eventually driving their kinetic energy to small values. This trend is monotonic in J_H. In (b), the farthest plane from the interface with the Ising spins, we find a much weaker effect, as is expected in the absence of direct contact with the classical spin layer. There is a steady increase of the absolute value of the kinetic energy- the opposite of the effect seen in layer $\ell = 0$. The sharp crossover temperature in the fermion kinetic energy aligns with T_c for the classical spins, as given in Fig. 3.

The double occupancy $\langle n_\uparrow n_\downarrow \rangle$ provides complementary information to the kinetic energy, and in particular provides insight into the formation of local moments $\langle m^2 \rangle$ and the possibility of Mott metal-insulator behavior. Specifically, $\langle m^2 \rangle = 1 - 2\langle n_\uparrow n_\downarrow \rangle$ at half-filling so that vanishing double occupancy implies a well-formed moment on every site, and a non-zero double occupancy implies moments which are partially suppressed by charge fluctuations. $\langle n_\uparrow n_\downarrow \rangle(T)$ is shown in Fig. 6. Data for plane 0 and plane 1 are shown in the top and bottom panels, respectively. In both cases $\langle n_\uparrow n_\downarrow \rangle$ takes on its uncorrelated value $\langle n_\uparrow n_\downarrow \rangle = \langle n_\uparrow \rangle \langle n_\downarrow \rangle = 1/4$ for $J_H = 0$, as should be the case for a metal with no interactions. In plane 0, there is a monotonic suppression of double occupancy with J_H, and hence a steady development of local moments. By the time $J_H = 4$ double occupancy has decreased to $\langle n_\uparrow n_\downarrow \rangle \sim 0.05$ implying $\langle m^2 \rangle(T) \sim 0.90$. The reason for this behavior is clear: the classical Ising spin S_i acts as a local magnetic field for the fermions on site i in plane 0, enhancing(suppressing) the occupation of the electron spin occupation parallel(antiparallel) to it. As we shall see, this induced moment formation aids in magnetic ordering.

In plane 1, more isolated from the classical spins, the double occupancy is barely modified from its $J_H = 0$

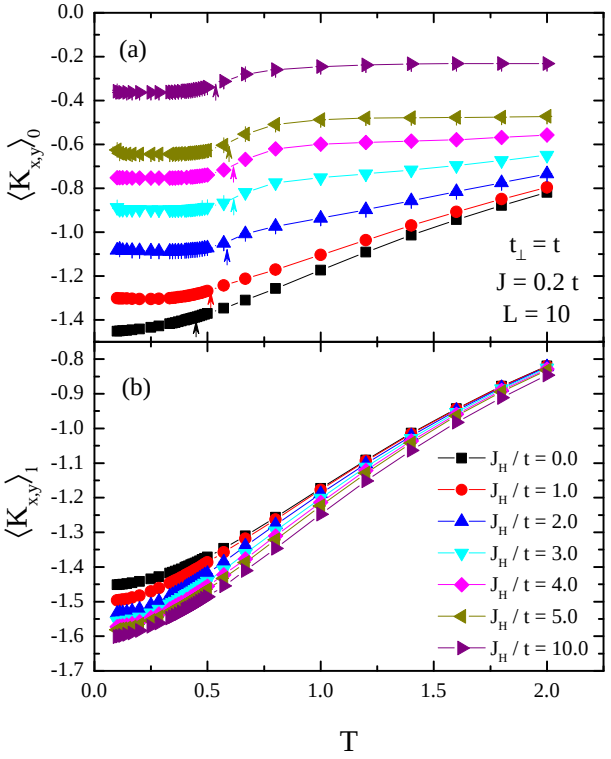

FIG. 5. (Color online) Intra-plane kinetic energy $\langle K\rangle$ as a function of temperature for different values of the interaction J_H. Here $t_\perp = t$: In (a) the fermionic plane $\ell = 0$ directly in contact with the Ising spin layer; and in (b) the more distant fermionic plane $\ell = 1$. The trend with increasing J_H is opposite in (a) and (b). For $\ell = 0$, the connection to the Ising spins reduces the kinetic energy at all temperatures. For $\ell = 1$, the kinetic energy increases. The vertical arrows at panel (a) indicate the critical temperature below which the magnetic ordering takes place for the Ising spins (Fig.3).

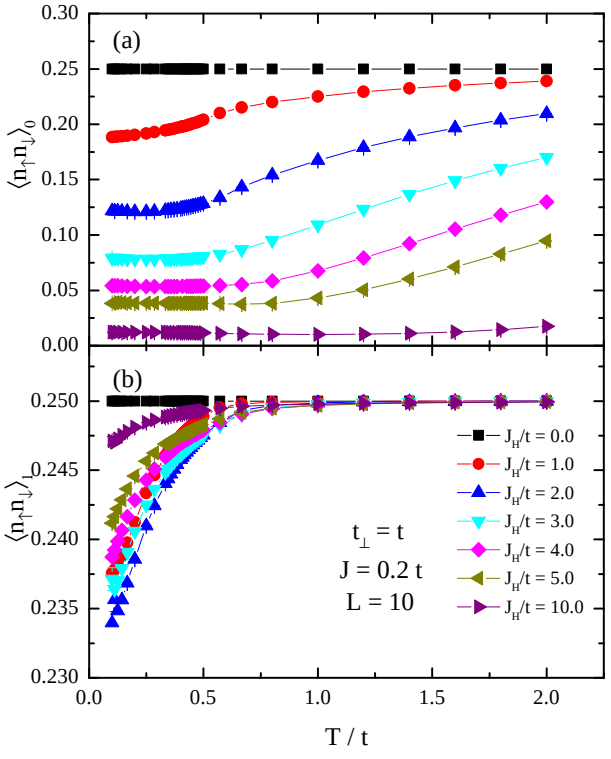

FIG. 6. (Color online) Temperature dependence of the double occupancy in the case $t_\perp = t$, in (a) for $\ell = 0$, while in (b) for $\ell = 1$. In the former, the increase of J_H decreases double occupancy since the electrons are strongly coupled to the Ising spins and, as a consequence, become more localized. For $\ell = 1$ the effect is very small (note the vertical scale) a slight decrease in double occupancy and then a recovery towards the $J_H = 0$ value which begins at $J_H/t \gtrsim 2$.

value. Nevertheless, despite exhibiting only a small efect, the onset of deviations provides a nice signal of the Neél transition temperature. Indeed, the non-monotonicity of $T_{\text{Néel}}$ observed in Fig. 3 is reflected in a similar non-monotonicity in the double occupancy in fermionic plane 1. Presumably, the large response of the double occupancy to the effective field in plane 0, which is evident far above $T_{\text{Néel}}$, masks the more subtle signature of the onset of long range order.

Long range order of the spin in the metallic planes can be analyzed by a finite size scaling of the antiferromagnetic structure factor,[26]

$$S^z_{\text{af}} = \frac{1}{L^2}\sum_{i,j}(-1)^{i+j}\langle s^z_i s^z_j\rangle = m^2_{\text{af},z} + \frac{A}{L} + \frac{B}{L^2} \qquad (5)$$

Here $m_{\text{af},z}$ represents the magnetic order parameter in the metallic layer, and the sum over i, j is restricted to that same layer. The coupling of the Ising spins with the z component of the fermionic spins breaks the $SU(2)$ symmetry of the Hubbard hamiltonian, leading to the possibility of long range order at finite temperature. Figure 7 shows the extrapolation according to Eq. 5. We chose $t_\perp = t$, and separate the contributions of plane 0 and 1 in (a) and (b), respectively. However, we do not attempt to discern this possibility, and restrict ourselves to examining the ground state magnetism by setting $T = t/10$ where the structure factor has saturated to its ground state value. The values of $m^2_{\text{af},z}$ in the two layers, obtained from the thermodynamic limit $1/L \to 0$ extrapolation, are displayed in Fig. 8 for the same three cases for the interplane hopping appearing in Fig. 3. Again, the plot is separated in (a) and (b) corresponding to the planes 0 and 1, respectively.

While plane 0, which directly interacts with the Ising spins, becomes easily "saturated" ($m_{\text{af},z} \to 1$) with the increase of J_H, the fermions on plane 1, farther from the classical spins, are less easily aligned. For smaller values of J_H, the long range-order present in the plane at the interface is propagated farther inwards. However, for $J_H/t \gtrsim 3.0$, the magnetism in plane 1 gets less robust. Indeed, the reduction of magnetic order in plane 1 coincides with saturation of magnetic order in plane 0.

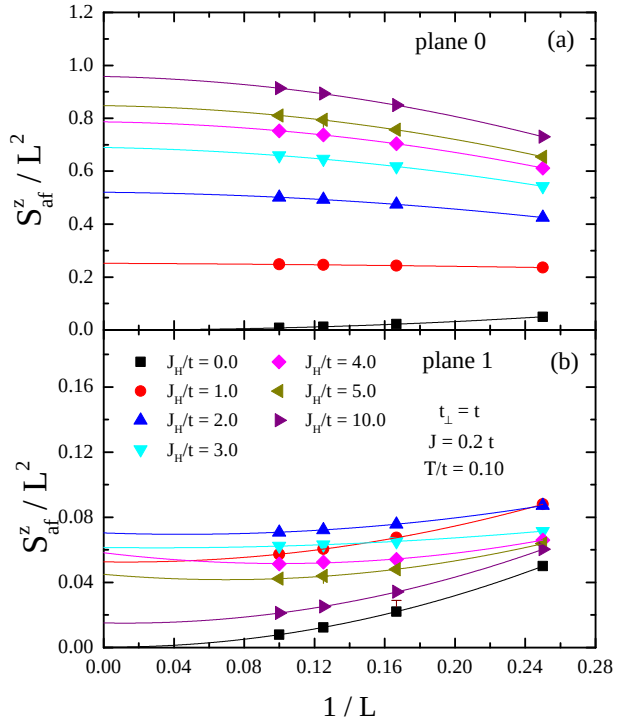

FIG. 7. (Color online) Finite size extrapolation for the z component of the antiferromagnetic structure factor $S^z_{\rm af}$ for planes 0 and 1, in (a) and (b), respectively. Here $t_\perp = t$ and $T/t = 0.10$. A parabolic fit is used to obtain the value in the thermodynamic limit, $m^2_{{\rm af},z}$.

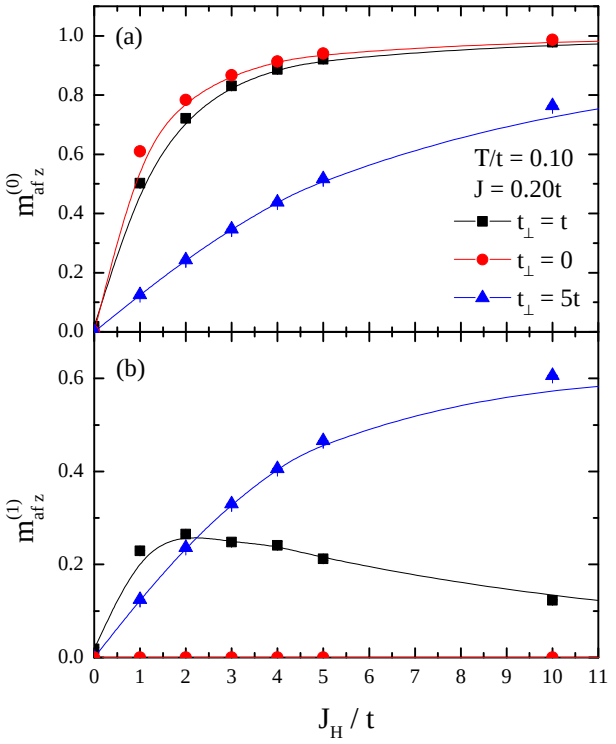

FIG. 8. (Color online) Antiferromagnetic order parameter as a function of J_H for temperature $T/t = 0.10$. In (a) for plane 0 and in (b) the same for plane 1. Plane 0 exhibits a rapid and monotonic saturation with J_H. $m^{(1)}_{{\rm af}\,z}$ in plane 1 first increases with J_H and then falls.

We turn now to the issue of how the coupling to the classical Ising spins affects the density of states $N(\omega)$ of the metal. There are two separate issues to consider. First, even at high temperatures, the fluctuating classical Ising spins act as a random site energy $\pm J_H$ for the fermions. In the limit $t = t_\perp = 0$, we expect $N(\omega) = \frac{1}{2}\big(\delta(\omega + J_H) + \delta(\omega - J_H)\big)$. Nonzero hopping will broaden this distribution. Second, as T is lowered, the Ising spins no longer fluctuate randomly but instead, for $J > 0$, form an ordered antiferromagnetic pattern. This staggered site energy opens a gap in the fermionic spectrum. Figure 9 shows $N(\omega)$ for $L = 12$ and $t_\perp = t$. The left panels give $N(\omega)$ in plane 0 for fixed $J_H/t = 3$ (the density of states for individual planes is obtained by the appropriate restriction of the spatial sum in Eq. 4.) and decreasing temperature. Both features discussed above are present: peaks in the density of states at $\pm J_H$ at all temperatures, and, near $\omega = 0$, an insulating gap which opens only below the Ising $T_c \sim 0.615$ (Fig. 2) for $J_H/t = 3$. The insulating gap is substantially less than one might expect from a strictly rigid staggered site energy. Presumably, this reflects some residual fluctuations of the Ising spins.

In the right panels of Fig. 9 the density of states in the plane further from the interface is shown. In the topmost panel Fig. 9(e), where $J_H = 0$, we recover the analytic result of the DOS of a bilayer with $t_\perp = t$ (displayed as a black thick curve), with some additional structure associated with the discrete finite lattice peaks. For J_H nonzero, the antiferromagnetic gap induced in layer 0 propagates to layer 1, rendering it insulating as well. The size of the gap in $N(\omega)$ for layer $\ell = 1$ goes down for large J_H, consistent with the decrease in the AF order parameter (Fig. 8(b)). One picture of the induced antiferromagnetism, and associated gap, in the layer not adjacent to the Ising spins, is the following: when the Ising spins order they induce antiferromagnetism in plane 0 via J_H. It is preferable to have a fermion in plane 1 of opposite spin from the one above it in plane 0, because it can then hop in the perpendicular direction, a lowering of the kinetic energy which is forbidden by the Pauli principle if the plane 1 fermion has parallel spin to the plane 0 fermion.

B. The ferromagnetic case

The antiferromagnetic tendency of tight binding electrons on a square lattice at half-filling can be understood from a weak coupling perspective: The Fermi surface is nested at the antiferromagnetic ordering vector (π, π) and, as a consequence, the non-interacting

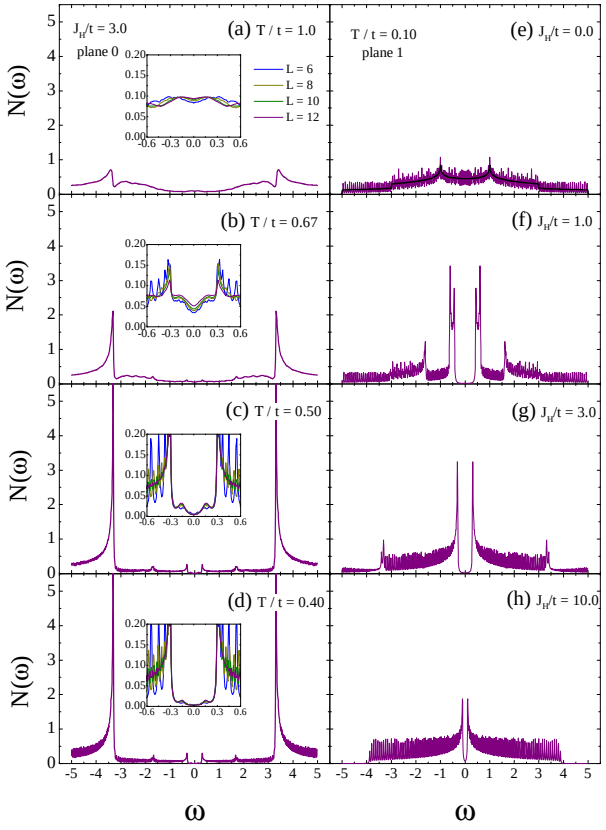

FIG. 9. (Color online) Left columns: Density of states $N(\omega)$ of fermions in plane 0 for different temperatures $T/t = 1.00, 0.67, 0.50, 0.40$ (a-d). The linear lattice size $L = 12$, Ising exchange coupling $J = 0.2t$, classical spin-fermion spin coupling $J_H = 3t$, and the interplane hopping $t_\perp = t$. There are two interesting features in $N(\omega)$: A pile-up of density at $\omega \sim \pm J_H$, which is present even at high T, and a gap which opens in the vicinity of $\omega = 0$ when T is decreased. Insets display the finite size dependence around $\omega = 0$. See text for further discussion. Right columns: Density of states $N(\omega)$ of fermions in plane 1 for different $J_H/t = 0.0, 1.0, 3.0, 10.0$ (e-h). The temperature $T/t = 0.10, t_\perp = t$, and $L = 12$. A gap is present for finite J_H, but gets filled for larger J_H. (See text for discussion.)

susceptibility

$$\chi_0(\mathbf{q}) = \frac{1}{L^2}\sum_{\mathbf{k}} \frac{f(\epsilon_{\mathbf{k}}) - f(\epsilon_{\mathbf{k+q}})}{\epsilon_{\mathbf{k+q}} - \epsilon_{\mathbf{k}}}, \qquad (6)$$

diverges there as $T \to 0$. This reasoning suggests T_c might be suppressed for ferromagnetically coupled Ising spins, whose ordering wave-vector conflicts with what the half-filled metallic fermion spins prefer.

Figure 10 shows the transition temperature T_c of ferromagnetically coupled Ising spins in contact with a half-filled metallic layer. It confirms that T_c is suppressed, consistent with the qualitative argument suggested above, and in contrast to the enhancement seen in the antiferromagnetic case of Fig. 3. The maximal

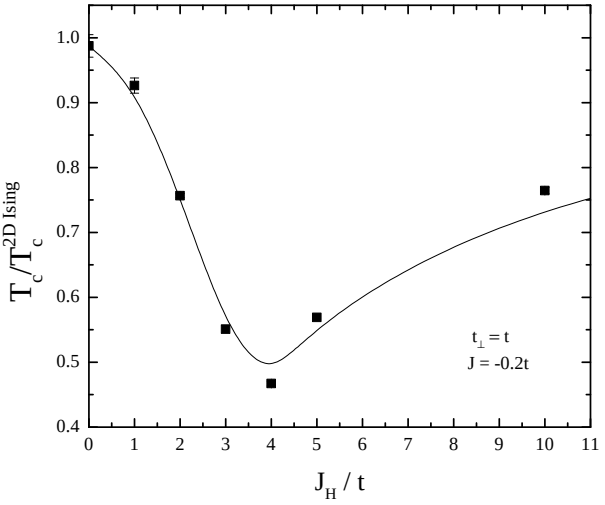

FIG. 10. (Color online) Curie temperature for the ferromagnetic Ising model with $J = -0.2t$ coupled with two fermionic planes ($t_\perp = t$), as a function of J_H. Unlike the antiferromagnetic case, the coupling with metal decreases the ferromagnetic critical temperature. Lines are guides to the eye.

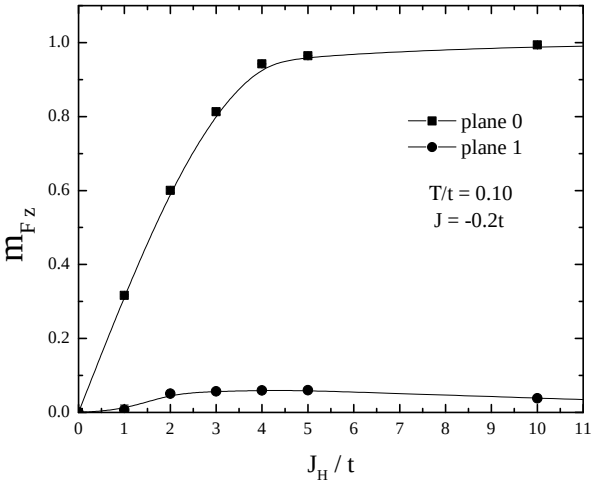

FIG. 11. (Color online) Dependence of the ferromagnetic order parameter m_F for the itinerant spins as a function of the interaction J_H with a ferromagnetic Ising plane. We choose temperature $T = t/10$. Here $t_\perp = t$ and $J = -0.2t$.

suppression of T_c occurs at $J_H/t \approx 4$, and reveals a lowering of T_c by almost a factor of two. T_c ultimately recovers, but only for very large values $J_H/t \gtrsim 5$.

When ferromagnetic order is present in layer 0, we can ask whether it will induce similar order in the more distant layer 1, something which occurred with antiferromagnetic coupling J. We calculated the

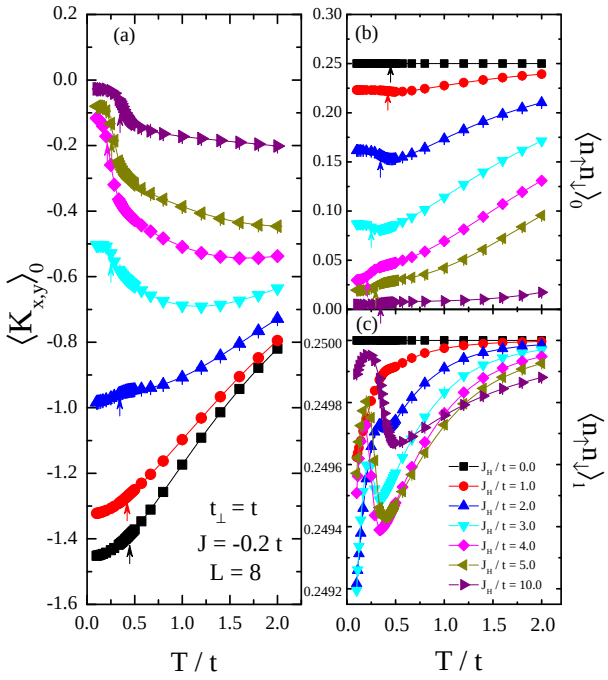

FIG. 12. (Color online) In (a), temperature dependence of the intra-plane kinetic energy for $\ell = 0$ in the case $t_\perp = t$ and ferromagnetic interaction between the Ising spins with exchange constant $J = -0.2t$. $J_H/t \gtrsim 3.0$ marks a distinct behavior where the kinetic energy decreases rapidly with decreasing temperature in opposition to the cases where J_H is small. Equivalently to Fig.6, the temperature dependence of the double occupancy in planes $\ell = 0$ and $\ell = 1$,(b) and (c), respectively. In the former, similar to the antiferromagnetic case, the increase in moment localization due to the interaction with the neighbor Ising spins can be readily seen. In the latter, despite the upturn of double occupancy for low temperatures and large interactions, the later downturn for even smaller temperatures indicates that the ferromagnetism of the Ising layers starts to propagate through the more distant fermionic region. Again, in panels (a) and (b), the vertical arrows depict the Ising critical temperature T_c.

ferromagnetic structure factor ($S^z_{\rm f} = (1/L^2)\sum_i \langle s^z_i s^z_j\rangle$) for the same values of interaction J_H considered in the previous case. A similar finite size analysis, Eq. 5, was performed, the order parameter m_F for *ferromagnetism* in each of the fermionic planes was obtained as function of J_H for low temperature, and is shown in Fig. 11. Ferromagnetic order is induced in both planes, although $m_{\rm f}$ is an order of magnitude smaller for plane 1 than for plane 0, in contrast to the antiferromagnetic case where there was only a factor of two difference.

As they order, the fermions in direct contact with the Ising spins ($\ell = 0$) start to localize as seen in their reduced double occupancy (Fig. 12(b)). For any J_H and T, the double occupancy for $\ell = 1$ is basically unchanged from its uncorrelated value 1/4 (Fig. 12(c)). This is similar to what happend in the AF case of Fig. 6(b). The behavior of the $\ell = 0$ kinetic energy (Fig. 12(a)), on the other hand, is quite different from the AF case (Fig. 5). Althougn in both cases there is a systematic suppression with J_H, in the ferromagnetic case the magnitude of the kinetic decreases as T is lowered for $J_H/t \gtrsim 3$. This is likely a consequence of the Pauli principle: In the F case, ordering of the Ising spins promotes polarization of the fermions in layer $\ell = 0$ and as this polarization becomes more and more complete the fermions can no longer hop on the lattice.

Finally, we analyze the influence of the magnetically ordered plane of Ising spins on the metallic density of states, Fig. 13. Similar to the AF case (Fig. 9), there are peaks at $\omega \sim \pm J_H$ for layer $\ell = 0$. The increase of J_H induces a pseudogap, however the insets to (c) and (d) indicate $N(\omega = 0)$ remains finite, in contrast to the AF case. The dashed line gives the density of states for a single fermionic plane coupled to a perfectly ordered ferromagnetic arrangement for the Ising spins, which is derived from the dispersion $E(\mathbf{k}) = -2t(\cos(k_x) + \cos(k_y)) \pm J_H$. The DOS for plane $\ell = 1$ is approximately given by that of a fermionic bilayer with $t_\perp = t$. The effect of J_H is to slowly decrease the distance between the van Hove singularities at $\omega = \pm t_\perp$. This trend would then ultimately result in a single van Hove singularity at $\omega = 0$ similar to that of an isolated free fermion plane. Increasing J_H helps "disconnecting" the planes $\ell > 0$ which are not right at the interface. Similar decoupling can be seen in layered Hubbard models[4].

IV. RESULTS- DOPED LATTICE

In the previous section we analyzed the influence in the critical temperature of the Ising plane after attaching a metal to it. Its enhancement(suppression) could be explained by the preferred wave-vector of the ordering in this metallic region. Since there is a natural tendency for short-ranged antiferromagnetic order for free fermions in a tightly-binded bipartite lattice at half-filling, these fermions and the Ising spins act cooperatively in order to boost the critical temperature of the antiferromagnetic Ising model. The same argument shows that when the Ising spins have a ferromagnetic coupling, the critical temperature is reduced, once again due to the antiferromagnetic tendency introduced by the contact with the fermionic spins. We now examine the doped lattice where the dominant AF response in the noninteracting $\chi_0(\mathbf{q})$ of Eq. 6 is no longer present.

Performing a similar analysis of Fig. 2 we computed the crossings in the Binder ratios for several values of the interaction J_H when the metal has a fixed total density $\rho = 0.87$. The global chemical potential μ in Eq. 1 is tuned in order to select this density for each of the lattice sizes and temperatures values calculated. Figure 14 shows the dependence of the critical value of the Ising spins for $t_\perp = t$ and $t_\perp = 0$. When $t_\perp = t$ so that two metallic layers are coupled to the Ising magnetic layer,

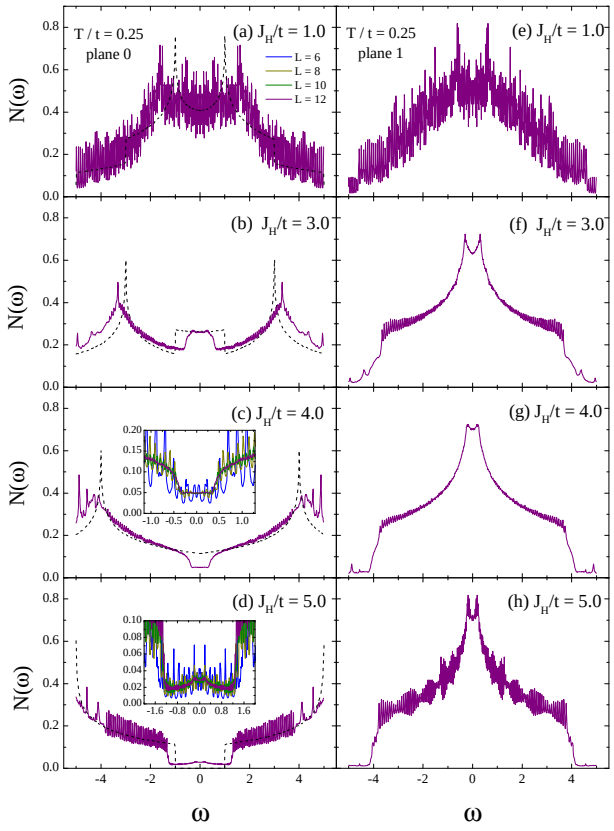

FIG. 13. (Color online) Density of states $N(\omega)$ of fermions in plane $\ell = 0$ for different values of the interaction $J_H/t = 1.0, 3.0, 4.0, 5.0$ (a-d) at temperature $T/t = 0.25$. Panels (e-h) show the correspondent results for plane $\ell = 1$. The linear lattice size is $L = 12$, Ising exchange coupling $J = -0.2t$ and the interplane hopping $t_\perp = t$. Insets at (c) and (d) include also $L = 6, 8$ and 10 near the region $\omega = 0$. Also displayed, as a dashed line, the corresponding density of states resulting from the dispersion of one plane under the influence of a fixed global chemical potential as if the configuration for the Ising spins is "frozen" in the ferromagnetic state. Worth noting is that there is a pile-up of density at $\omega \sim \pm J_H$, and a pseudogap which opens only for values of $J_H/t \gtrsim 4$. Insets in (c) and (d) show a finite size comparison of this gap.

the qualitative behavior is similar to that at half-filling (Figs. 3 and 10). Indeed, the values of the transition temperatures are quantitatively similar. This is true in both the ferromagnetic and antiferromagnetic cases.

However, when $t_\perp = 0$, so that only one metallic plane is coupled, doping appears to change the behavior of T_c quite substantially. While for small values of J_H the increase(decrease) of the critical temperature of the antiferromagnetic(ferromagnetic) Ising model is the same as for $\rho = 1$, once higher values of J_H are reached ($J_H/t \sim 4$ in the AF case and $J_H/t \sim 10$ in the F one) the scenario changes. An antiferromagnetic Ising plane has its critical temperature decreased by the coupling with the free electron spins while in the ferromagnetic case the critical temperature is enhanced. This is not completely

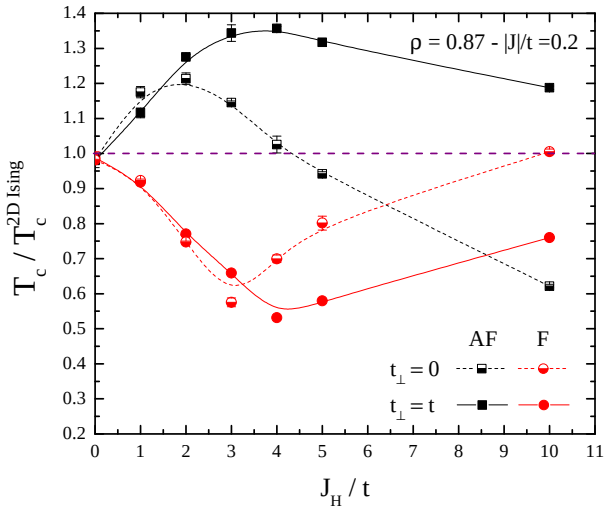

FIG. 14. (Color online) Dependence of critical temperature on J_H of the long-range order for the Ising spins when coupled to fermions at total density $\rho = 0.87$ for different scenarios: antiferromagnetic(ferromagnetic) interaction between the Ising spins and two fermionic planes coupled by a hopping $t_\perp = t$ and the same for the interaction with a single plane. In the situation one have two fermionic planes, this dependence is quantitatively similar to the half-filled case. In the latter scenario, in the regime of larger interactions, the coupling with the fermions is detrimental (benign) to the critical temperature when the antiferromagnetic(ferromagnetic) Ising model is considered in a clear contrast with the half-filled case.

unexpected since, as commented earlier, the peak in $\chi_0(\mathbf{q})$ moves away from (π, π) so that the fermions in the metal no longer so strongly favor AF order.

The reason that this does not happen in the two layer case $t_\perp = 1$ is that the second metallic layer $\ell = 1$ acts as a charge reservoir for the layer $\ell = 0$ at the interface. That is, the electron density is imbalanced, as seen in Fig. 15. Plane $\ell = 0$ adjacent to the magnetic layer has a tendency to become half-filled, leaving the farthest plane less populated. For larger values of J_H the occupations tend to 1.0 and 0.75, for $\ell = 0$ and $\ell = 1$ respectively. Throughout this evolution the total density is preserved at $\rho = 0.87$. The half-filling of layer $\ell = 0$ allows for the enhancement(supressing) of the critical temperature of an antiferromagnetic(ferromagnetic) aligned Ising plane.

V. CONCLUSION

We studied magnetic order at the interface between an insulator and a metal using quantum Monte Carlo. Specifically, we considered a 2D Ising plane coupled to a lattice of noninteracting (metallic) fermions. In the case of an antiferromagnetic Ising model, and a half-filled metal, the coupling enhanced the Ising critical temperature. Antiferromagnetic order was also induced

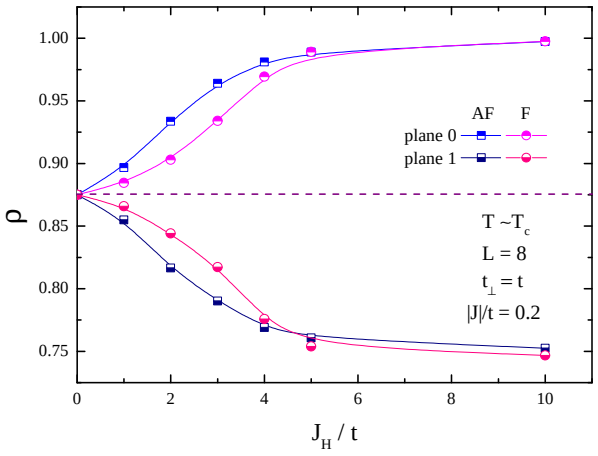

FIG. 15. (Color online) Dependence of the density on J_H/t in each of the fermionic planes at temperatures close to where the magnetic transition takes place for the Ising spins. The lattice size is $L = 8$, $t_\perp = t$ and the interaction among the Ising spins are either ferro or antiferromagnetic with value $|J| = 0.2t$.

in the metal, both in the layer immediately at the interface with the classical spins and also deeper within. This enhancement occurs even in the case where the interlayer hopping in the fermionic sheet is made large enough that the fermions become a band insulator, namely a bilayer with interplane hopping $t_\perp$ bigger that $4t$.

In contrast, the critical temperature of ferromagnetic Ising spins is reduced by the coupling to the fermions at half-filling. We attribute these distinct effects to be a consequence of the perfect nesting of the square lattice fermion tight binding hamiltonian, which favors antiferromagnetism. Indeed, studies of the doped lattice demonstrate that the system's desire to optimize 'magnetic consistency', that is to have an AF metallic response when the magnetic layer is AF, is so great that, if available, charge will be pulled from a second magnetic layer into the interface metallic layer so that half-filling is maintained there. In the absence of such a reservoir, the AF transition is suppressed by this mismatch with the metallic ordering vave vector.

A central consideration of our work has been the consistency of the order in the classical spin plane from the ordering tendency of the metal. In "unfrustrated" cases where the metal and local spins prefer the same wave-vector, transition temperatures are enhanced, and *vice versa*. Recent experiments[27] have explored the importance of these considerations on the decoupling of surface and bulk magnetism in UO_2. The distinct surface behavior observed is attributed to the different symmetry of its ordered phase relative to the bulk. Other 3D systems in which 2D order occurs due to frustration are certain of the doped cuprate superconductors[28,29]. In individual CuO_2 sheets, stripes of d-wave order coexist with intervening antiferromagnetic stripes. The orientation of the d-wave phases alternates from stripe to stripe in a given layer. In adjacent CuO_2 sheets, the same stripe pattern occurs, but, because of structural effects, the stripes are oriented perpendicular to the neighboring sheet. The result is that the intersheet Josephson coupling tends to cancel and 2D superconductivity is observed.

A natural progression of the work reported here would be to consider the case of continuous XY (planar) or Heisenberg spins. As previously noted, in this case an isolated 2D spin plane has no transition to long range order, owing to the Mermin-Wagner theorem. One interesting question will be how the less robust power law correlations which develop at low T in the XY case are qualitatively affected by coupling to the metal. For $J < 0$, where we find the Ising T_c suppressed, will the Kosterlitz-Thouless transition survive? Because the fermion determinant depends only on the spin degrees of freedom in the interface layer, adding additional spin layers has relatively little computational cost. Thus it is feasible to study a 3D lattice Heisenberg spins, which has a finite ordering temperature, coupled to one of more metallic layers.

Acknowledgements: This work was supported by DOE DE-NA0001842-0, and by the Office of the President of the University of California. Support from CNPq (TP and RM), FAPERJ (TP), and the CNPq Science Without Borders project (RS) is gratefully acknowledged.

[1] M. Troyer, H. Kontani, and K. Ueda, Phys. Rev. Lett. 76, 3822 (1996).
[2] A.W. Sandvik and D.J. Scalapino, Phys. Rev. Lett. 72, 2777 (1994).
[3] R.T. Scalettar, J.W. Cannon, D.J. Scalapino, and R.L. Sugar, Phys. Rev. B50, 13419 (1994).
[4] A. Euverte, F. Hebert, S. Chiesa, R.T. Scalettar, and G.G. Batrouni, Phys. Rev. Lett. 108, 246401 (2012).
[5] E. Dagotto, T. Hotta, and A. Moreo, Phys. Rep. 344, 1 (2001).
[6] W. Lv, F. Krüger, and P. Phillips, Phys. Rev. B82, 045125 (2010).
[7] W.-G. Yin, C.-C. Lee, and W. Ku, Phys. Rev. Lett. 105, 107004 (2010).
[8] S. Liang, G. Alvarez, C. Sen, A. Moreo, and E. Dagotto, Phys. Rev. Lett. **109**, 047001 (2012).
[9] K. S. Takahashi, M. Kawasaki, and Y. Tokura, Appl. Phys. Lett. **79**, 1324 (2001).
[10] J. W. Freeland, J. Chakhalian, A. V. Boris, J.-M. Tonnerre, J. J. Kavich, P. Yordanov, S. Grenier, P.

Zschack, E. Karapetrova, P. Popovich, H. N. Lee, and B. Keimer, Phys. Rev. B**81**, 094414 (2010).
[11] H. Tan, R. Egoavil, A. Béché, G. T. Martinez, S.VanAert, J. Verbeeck, G. VanTendeloo, H. Rotella, P. Boullay, A. Pautrat, and W. Prellier, Phys. Rev. B**88**, 155123 (2013).
[12] A. Mukherjee, N. D. Patel, S. Dong, S. Johnston, Adriana Moreo, and Elbio Dagotto, arXiv:1409.6790.
[13] We focus here in the penetration of the classical spin order into the metal, and hence have a single spin layer and multiple metallic layers.
[14] A detailed discussion of mean field treatments and the role of rotationally symmetric decouplings in the context of layered Hubbard models is contained in J. Xu, S. Chiesa, E.J. Walter, and S. Zhang, J. Phys. Cond. Mat. 25, 415602 (2013).
[15] F.C. Zhang and T. M. Rice, Phys. Rev. B37, 3759 (1988); C. Gros, R. Joynt, and T.M. Rice, *ibid.* 36, 381 (1987).
[16] This real-valued matrix turns into a complex one once we define the complex phases in the hopping terms to reduce the finite size effects.
[17] Y. Motome and N. Furukawa, J. Phys. Soc. Japan 68, 3853 (1999).
[18] G. Alvarez, C. Sen, N. Furukawa, Y. Motome, and E. Dagotto, Comp. Phys. Comm. 168, 32 (2005).
[19] C. Sen, G. Alvarez, Y. Motome, N. Furukawa, I. A. Sergienko, T. C. Schulthess, A. Moreo, and E. Dagotto, Phys. Rev. B73, 224430 (2006).
[20] K. Binder, Zeitschrift für Physik B Condensed Matter 43, 119 (1981).
[21] J. Tinka Gammel, D. K. Campbell, and E. Y. Loh, arXiv:cond-mat/9209026.
[22] C. Gros, Phys. Rev. B53, 6865 (1996).
[23] S. Chiesa, P.B. Chakraborty, W.E. Pickett, and R.T. Scalettar, Phys. Rev. Lett. 101, 086401 (2008).
[24] F. F. Assaad, in *Quantum Simulations of Complex Many-Body Systems: From Theory to Algorithms*, edited by J. Grotendorst, D. Marx, and A. Muramatsu (John von Neumann Institute for Computing (NIC), 2002), Vol. 10, pp. 99-155.
[25] The kinetic energy does not vanish even in the Mott insulator owing to quantum fluctuations. See, for example, S.R. White, D.J. Scalapino, R.L. Sugar, E.Y. Loh, J.E. Gubernatis, and R.T. Scalettar, Phys. Rev. B40, 506 (1989); and C.N. Varney, C.R. Lee, Z.J. Bai, S. Chiesa, M. Jarrell, and R.T. Scalettar, Phys. Rev. B80, 075116 (2009).
[26] Finite size scaling of the farthest distance spin correlation can also be done, and leads to the same value for the order parameter. In general the structure factor has the advantage of smaller statistical error bars, but the disadvantage of larger finite size effects (a bigger value of the parameter A in Eq. 5).
[27] S. Langridge, G.M. Watson, D. Gibbs, J.J. Betouras, N.I. Gidopoulos, F. Pollmann, M.W. Long, C. Vettier, and G.H. Lander, Phys. Rev. Lett. 112, 167201 (2014).
[28] J.M. Tranquada, Physica B407, 1771 (2012).
[29] Z. Stegen, Su Jung Han, Jie Wu, A K. Pramanik, M. Hücker, Genda Gu, Qiang Li, J.H. Park, G.S. Boebinger, and J.M. Tranquada, Phys. Rev. B87, 064509 (2013).